CNWRA *A center of excellence in earth sciences and engineering*

A Division of Southwest Research Institute™
6220 Culebra Road • San Antonio, Texas, U.S.A. 78228-5166
(210) 522-5160 • Fax (210) 522-5155

February 26, 2002
Contract No. NRC–02–97–009
Account No. 20.01402.871

U.S. Nuclear Regulatory Commission
ATTN: Dr. John W. Bradbury
Division of Waste Management
Two White Flint North
Mail Stop 7F-13
Washington, DC 20555

Subject: Subject: Transmittal of "Colloid Facilitated Transport Modeling—Journal Paper" (IM 20.01402.871.220)

Dear Dr. Bradbury:

This letter transmits Intermediate Milestone 20.01402.871.220 "Colloid Facilitated Transport Modeling—Journal Paper." This item is identified in the FY2002 CNWRA Operations Plans as a deliverable for the Radionuclide Transport Key Technical Issue. The publication title of this manuscript is "Significance of Kinetics for Sorption on Inorganic Colloids: Modeling and Experiment Interpretation Issues."

As you know, DOE models for radionuclide transport at Yucca Mountain predict Pu transport via colloids. These Pu-bearing colloids significantly contribute to calculated doses at long time frames. The manuscript transmitted by this letter describes independent models of colloid transport CNWRA has developed as tools to support NRC responsibilities to evaluate the DOE approach. This work is part of ongoing issue resolution activities under the Radionuclide Transport Key Technical Issue.

The approach presented in this manuscript has been used to evaluate data requirements for long-term predictive calculations of colloid facilitated transport and to evaluate laboratory kinetic sorption data for colloids. This model is expected to be useful for interpreting laboratory data where indications are found for kinetic behavior occurring on widely separated time scales. Related models may also be useful in testing DOE abstractions of transport models to field scales for performance assessments.

Washington Office • Twinbrook Metro Plaza #210
12300 Twinbrook Parkway • Rockville, Maryland 20852-1606

If you have any questions about this deliverable, please contact me (210.522.5540) or Dr. Scott Painter (210.522.3348).

Sincerely,

English C. Pearcy, Manager
Geohydrology and Geochemistry

/ph
Enclosure
cc:

J. Linehan	N. Coleman	W. Patrick
D. DeMarco	H. Arlt	CNWRA Directors
E. Whitt	W. Ford	CNWRA Element Mgrs
B. Meehan	L. Hamdan	T. Nagy (SwRI contracts)
J. Greeves	D. Brooks	P. Maldonado
W. Reamer	B. Leslie	S. Painter
J. Schlueter	J. Pohle	D. Turner
K. Stablein	E. Esh	D. Pickett
J. Ciocco	B. Dam	
A. Campbell		

Significance of kinetics for sorption on inorganic colloids: Modeling and experiment interpretation issues

S. Painter * V. Cvetkovic† D. Pickett* D.R. Turner*

February 13, 2002

Abstract

A two-site kinetic model for sorption on inorganic colloids is developed. The model quantifies linear first-order sorption on two types of sites ("fast" and "slow") characterized by two pairs of rates (forward and reverse). We use the model to explore data requirements for long-term predictive calculations of colloid-facilitated transport and to evaluate laboratory kinetic sorption data of Lu et al. (1,2). Five batch sorption data sets are considered with plutonium as the tracer and montmorillonite, hematite, silica, and smectite as colloids. Using asymptotic results applicable on the time scale of limited duration experiments, a robust estimation procedure is developed for the fast-site partitioning coefficient K_c and the slow forward rate α. The estimated range of K_c is 1.1–76 L/g, the range for α is 0.0017–0.02 1/h. The fast reverse rate k_r is estimated in the range 0.012–0.1 1/h. Comparison of one-site and two-site sorption interpretations reveals the difficulty in discriminating between the two models for montmorillonite and to a lesser extent for hematite. For silica and smectite, the two-site model clearly provides a better representation of the data as compared with a single site model. Kinetic data for silica are available for different colloid concentrations (0.2 g/L and 1 g/L). For the range of experimental conditions considered, α appears to be independent of colloid concentration.

*Center for Nuclear Waste Regulatory Analyses; Southwest Research Institute; San Antonio, TX, USA

†Division of Water Resources Engineering; Department of Civil and Environmental Engineering; Royal Institute of Technology; Stockholm, Sweden

1 Introduction

Many of the groundwater contaminants that interact strongly with soils and aquifer rocks also have a strong affinity for the colloidal particles of various origins that are widely observed in groundwaters (3–5). In the absence of colloids, these strongly sorbing contaminants would be relatively immobile in the subsurface, but once bound to colloids they can potentially be transported great distances with flowing groundwater. Although this process of colloid-facilitated tranport is of general interest in contaminant hydrology, it is particularly relevant to studies of long-term geological disposal of high-level nuclear waste. Most countries that are currently investigating geological disposal endorse a multiple barrier approach that includes both engineered and natural barriers to radionuclide release (6). Colloid-facilitated transport is one mechanism that could potentially affect the performance of the natural geological barriers.

In the United States, the Nuclear Waste Policy Act of 1982 (as amended 1987) charges the U.S. Department of Energy (DOE) with characterizing and evaluating Yucca Mountain, Nevada as a potential site for a geologic high-level waste repository. As part of a license application to the U.S. Nuclear Regulatory Commission, the DOE is to demonstrate the long-term performance of any proposed nuclear waste repository. Total system performance assessments (7), undertaken as part of the DOE's evaluation of the potential repository, reveal colloid faciliated transport to be an important factor controlling dose to the receptor group. For example, calculations suggest that colloidal release and transport of 239Pu is the second largest contributor to total dose at 70,000 years after permanent closure. At 100,000 years, colloidal 239Pu is estimated to contribute 25 percent of the total dose (7).

To date, most of the DOE efforts to model colloid transport have focused on plutonium. Performance assessment sensitivity analyses suggest that colloid transport may also have an impact on strongly sorbing elements such as thorium and americium, but only to the extent that radionuclide sorption onto colloids is irreversible (8). If sorption on colloids is reversible and relatively rapid, then the effect of colloid-facilitated transport is for most practical purposes negligible, given the relatively low colloid concentrations typically found in aquifers. The role played by colloids in subsurface contaminant transport is significant only if binding to colloids is irreversible (or slowly reversible) relative to the time scale of the transport problem. Understanding and characterizing the kinetics of sorption on colloids is thus critical to obtaining accurate assessments of colloid-facilitated transport in groundwater.

Irreversible (or slowly reversible) sorption of plutonium on inorganic colloids has been suspected in relation to a few field observations (e.g., (9)). Of particular interest is the fact that plutonium associated with natural colloids detected at the Nevada Test Site appeared to be irreversibly attached to colloids (10). In spite of these field-scale indications, verifying irreversible or slowly reversible sorption under laboratory conditions is difficult because the time scales required for observation may be prohibitive. Perhaps the most comprehensive data sets for sorption on colloids under laboratory conditions was presented by Lu et al. (1,2). The laboratory studies of Lu and co-workers include

kinetic sorption data up to 240 hours. In most cases steady-state was not reached during this time. Thus the data of Lu et al. are of potential interest for assessing slow sorption, if such can be identified.

In this study, we present a phenomenological sorption model for interpreting results of laboratory experiments carried out in a batch or flow-through reactor. Using the proposed model, we re-evaluate sorption data of Lu et al. (1,2) for plutonium on four colloid types (hematite, montmorillonite, silica and smectite). We present indications of kinetics governed by two distinct time scales, and estimate ranges of the kinetic rates. In addition, we address the important issues of model discrimination and uncertainties in estimation of sorption rates. Our motivation, in addition to the basic scientific questions associated with colloid sorption kinetics, is to understand data requirements for model discrimination, validation, and calibration. Specifically, we use the model to explore how uncertainties associated with the interpretation of a limited-duration laboratory experiment propogate into uncertainties in predictive calculations of colloid-facilitated transport.

2 Two-site model for colloid sorption kinetics

We consider a flow-through reactor with an aqueous solution which contains colloids; water and colloid flow is assumed to be at steady-state. The reactor is either a two-phase system (aqueous solution – colloids), or a three-phase system (aqueous solution – colloids – immobile porous matrix). The turnover rate in the reactor is $\omega \equiv 1/\Delta\tau$ [T^{-1}] where $\Delta\tau$ is the turnover time. A tracer mass M_0 [M] is injected into the flow reactor with a time-dependent rate $\varphi(t)$ [T^{-1}]; for a pulse $\varphi(t) = \delta(t)$.

Rather than attempt to model in a mechanistic way all of the physical and chemical processes that cause sorption on colloidal particles, we adopt a phenomenological approach and assume that sorption takes place on two types of sites: "fast sites" where sorption is relatively rapid, and "slow sites" where sorption takes place over a relatively long time. Multiple sites on colloids have been assumed in earlier studies for interpreting laboratory data on colloid-facilitated transport (e.g. (11)), as well as for field-scale transport (e.g., (12)).

Let X [M] denote tracer mass in the solution, Y [M] tracer mass attached to the fast sites on colloids, and Z [M] tracer mass attached to the slow sites on colloids. The mass balance equations for X, Y and Z are written as:

$$
\begin{aligned}
R\frac{dX}{dt} &= -\omega X + M_0\,\varphi(t) - k_f\,X + k_r\,Y - \alpha X + \beta Z - \lambda R X \\
\frac{dY}{dt} &= -\omega Y + k_f\,X - k_r\,Y - \lambda Y \qquad (1)\\
\frac{dZ}{dt} &= -\omega Z + \alpha X - \beta Z - \lambda Z
\end{aligned}
$$

where $R \equiv 1 + (1-\theta)\rho K_d/\theta$ is the retardation coefficient for the porous matrix (if the reactor is a three-phase system) with θ being the porosity and ρ [ML^{-3}] the solid phase

density. Thus if a porous matrix is present, we assume linear equilibrium sorption with a sorption coefficient K_d [L^3M^{-1}]. If the flow reactor is a two-phase system, then $\theta = 1$ and $R = 1$. The rates k_f [T^{-1}] and k_r [T^{-1}] are forward and reverse rates for sorption on fast sites on colloids, α [T^{-1}] and β [T^{-1}] are the slow forward and reverse rates for the colloids, and λ [T^{-1}] is the tracer decay rate. We denote the ratio $k_f/k_r = C_c K_c$ where C_c [ML^{-3}] is the colloid concentration, and K_c [L^3M^{-1}] is the partitioning coefficient for the fast sites once equilibrium is reached.

A number of special cases of interest can be deduced from eq 1. For $\omega = 0$ we obtain a system of mass balance equations for a batch reactor where $X_0 = M_0/R$ is the tracer mass in solution at time $t = 0$, and $\varphi(t) = \delta(t)$. If k_r is large relative to ω (reactor case), or relative to the experimental time (batch experiment), we may approximate sorption on fast sites as equilibrium. If β is small relative to ω (reactor case), or relative to the experimental time (batch experiment), then sorption on slow sites may be approximated as irreversible by setting $\beta = 0$.

Analytical solutions of eq 1 relevant for our following discussions are summarized in the Appendix.

3 Effect of slow kinetics on colloid-facilitated transport

We use the flow-through reactor model eq 6 to illustrate the potential impact of colloids. Although this zero-dimensional model is strictly applicable only to a well-mixed system and not to a real aquifer system, it still provides some general insights into sensitivities under field conditions. We consider plutonium as a tracer and calculate the discharge from the flow reactor as a function of time using basic transport parameters that are consistent with previous representations of the alluvial aquifer near Yucca Mountain, Nevada (13,12). For this example, we assume $\theta = 0.3$ for porosity, and $\rho = 2400$ kg m^{-3} for density. The mean sorption coefficient for plutonium on the aquifer grains is $K_d = 5$ m^3 kg^{-1}; we assume the same value to be applicable for colloids, i.e., $K_c = K_d$. We also use a turnover rate of $\omega = 2.5 \times 10^{-4}$ yr^{-1} which corresponds to a mean residence time of 4000 years. The colloidal concentration in the aquifer is assumed as $C_c = 20$ mg L^{-1}, which is presumably an upper limit based on available data. The half-life of plutonium is 2.4×10^4 yr from which we deduce λ.

The total mass in the system at any given time is $RX + Y + Z$. In the absence of sorption on the porous matrix ($R = 1$), the total mass in the system is exponentially decaying and the discharge from the system is $M_0\omega \exp(-\lambda t - \omega t)$, irrespective of the colloid sorption behavior. In the case with no colloids, the discharge from the system is ωX_{eq}, where $X_{eq}(t) = M_0 \exp(-\omega t/R - \lambda t)/R$. These are the two limiting situations. If the tracer sorbs on the porous matrix and colloids are present, the colloids partially defeat the retention properties of the matrix and the discharge will be somewhere between the two limiting cases. In this situation it is necessary to solve the full system eq 1 to obtain the discharge (see the Appendix).

Figure 1a illustrates the dimensionless Pu mass $(X+Y+Z)/X_{eq}$ discharged from the flow reactor as a function of time for different dimensionless sorption rates α/ω and assuming $\beta = 0$. In Figure 1b we show the peak of $(X+Y+Z)$ normalized with X_{eq} at peak times, as a function of α/ω and β/ω. Values of $(X+Y+Z)/X_{eq}$ that are close to unity in Figure 1b indicate small impact of colloids; increasing deviation from unity indicates an increasing impact of colloids.

Figure 1 clearly illustrates the importance of slow kinetics. The largest effect of colloids is for $\beta/\omega = 0$, which in practice implies approximately $\beta/\omega < 1$ (Figure 1b). Hence, for $\beta/\omega < 1$, sorption on slow sites may be approximated as irreversible. Larger α/ω combined with small β implies a larger peak of Pu breakthrough. As β/ω increases, the impact decreases, converging asymptotically to the equilibrium case.

4 Comparision with kinetic sorption experiments

4.1 Experiments and data

A series of laboratory tests were carried out at the Los Alamos National Laboratory by Lu and co-workers with the purpose of studying sorption on colloids (1,2). Colloids of different minerals were considered (hematite, smectite, montmorillonite, silica), with four different actinides (plutonium, americium, neptunium and uranium), in two types of water samples (natural and synthetic), with varying colloid concentration (from 0.05 to 1 g/L), temperature (20, 40, and 80^0C), and ionic strength (from 0.005 M to 0.134 M). The kinetics of sorption in the experiments reported by Lu et al. (1,2) were recorded up to 10 days.

We focus here on sorption of plutonium in natural groundwater samples at the "base case" conditions: particle size in the range 70-100 nm, ionic strength of 0.005 M, temperature of 20^0C and pH of 8.2. In the three tests for hematite, montmorillonite and silica reported in 2000, the colloid concentration C_c is 0.2 g/L, whereas in the two tests for smectite and silica reported in 1998,[1] the colloid concentration is 1 g/L. We note that the sorption kinetic data base of Lu et al. (1,2) is most extensive for Pu(V). Furthermore, irreversible sorption of plutonium on colloids has been suspected in several field observations (e.g., (9,10)). Thus plutonium is of particular interest.

The adsorbed Pu(V) fraction (denoted by ϕ) was measured at the following times: 1, 4, 24, 48, 96 and 240 h. The adsorbed fraction as a function of time is summarized in Table 1 with error bounds. The ϕ data summarized in Table 1 were interpreted by Lu et al. (1,2) assuming a linear equilibrium sorption model. The values of K_c obtained from data in Table 1 as estimated by the equilibrium sorption model, are summarized in Table 2.

An important aspect of the data in Table 1 is that sorption has apparently not reached steady-state (equilibrium) conditions during the 240 hours of the experiment; the last few data points indicate a positive gradient in $\phi(t)$ for all five tests. In the following, we

[1] Additional minerals were considered in Lu et al. (1), but the kinetic data for these minerals is for a shorter time interval.

re-evaluate the data in Table 1 accounting for fast and slow sorption kinetics as defined by the two-site kinetic model eq 1.

4.2 Results

The basic assumption here is that β is small such that slow sorption can be considered irreversible over the duration of the experiments (240 h); thus eq 8 is applicable. Our evaluation strategy consists of two steps. First, we estimate the two parameters K_c and α using the asymptotic result eq 10. Eq 10 neglects the kinetics of sorption on fast sites, whereas it is obvious from the data that non-equilibrium conditions prevail in the initial phase of the experiments; hence 10 provides a robust estimate of K_c and α. Next, we use eq 8 with $C_cK_c(\equiv k_f/k_r)$ and α as obtained in the first step, and calibrate the reverse rate on the fast sites, k_r, to produce the best fit with the data. The obtained parameters K_c, α and k_r from the two steps are summarized in Table 3 for the five data sets.

The best fit curves are compared to the data in Figure 3. The best fits with the one-site and two-site models are also compared in Figure 3; calibrated parameters for the one-site model are summarized in Table 2. Note that the measurement errors as summarized in Table 1 are relatively small (comparable to the symbol size for most points in Figure 3), and is neglected in the parameter estimation.

Hematite

Hematite is characterized by a relatively rapid increase in the adsorbed Pu fraction ϕ followed by an apparently slow increase. Judging by the eye, the one- and two-site models provide similar matches with the data. The key difference in the two interpretations is that the one-site model attains a steady-state at approximately 30 h, and thus does not capture the slight but important increase in ϕ in the range $30 < t < 240$ h. We emphasize that this increase is well outside the error bounds: ϕ increases by 1.8% from 48 h to 240 h, whereas the error margin at 240 h is 0.17%. The third data point (at 24 h) is apparently an outlier with respect to both models. The estimates of K_c by the two models vary between 15-20%, i.e., from 76-110 L/g (Tables 2 and 3).

Montmorillonite

For montmorillonite, the fast kinetic effects seem to extend over the entire range $t \leq 240$ h. Thus eq 10 is not applicable and is used here for comparative purposes only. The two sorption models provide an equally close match with the data, with the fourth data point (48 h) being an outlier for both models. The estimates of K_c by the two models vary by a factor of 2, 3.1 to 6 L/g (Tables 2 and 3).

Silica

Data for sorption on colloidal silica are available at two colloid concentrations: $C_c = 0.2$ g/L and $C_c = 1$ g/L. Whereas data for silica with $C_c = 0.2$ g/L is characterized by a

relatively large k_r (0.1 1/h, Table 3), implying that fast kinetic effects that are limited to the range $t < 20 - 30$ h, data for $C_c = 1$ g/L is characterized by a lower k_r (0.035 1/h, Table 3) implying that fast kinetic effects extend over a longer time. The data set for $C_c = 0.2$ g/L exhibits a clear linear increase in ϕ in the range $24 \leq t \leq 240$ h, hence estimates using eq 10 are based on all four data points. Since the linear increase of ϕ is not apparent for the data set with $C_c = 1$ g/L, we used the estimate of α and K_cC_c from the $C_c = 0.2$ g/L data set ($\alpha = 0.0018$ 1/h and $K_cC_c = 1.1$, Table 3); this implies that α is assumed independent of C_c, in contrast to K_c. Such an extension is justified by the fact that slopes of the two last data points are almost identical for the two data sets (Figure 3 for silica).

The two-site model provides a close match with the data for the smaller value of C_c and provides a reasonably good match for the $C_c = 1$ g/L situation. The one-site model provides a good fit for only the last two data points in the $C_c = 0.2$ g/L situation. For the $C_c = 1$ g/L situation, the one-site model (thin dashed curve in Figure 3 for silica) provides a good fit for the last data points, but fails to capture the rapid initial increase in ϕ.

The estimated parameter values for silica in Table 3 provide some indication of how the parameters might depend on C_c. This is of particular interest because C_c is usually considerably smaller under field conditions as compared with the laboratory conditions used by Lu et al. (1,2). The most apparent difference in the two data sets is that K_c is larger by roughly a factor of five for $C_c = 0.2$ g/L as compared to the $C_c = 1$ g/L case. This type of dependence of K_c on C_c is consistent with a more general trend reported in Lu et al. (1,2), where several values of C_c ranging from 0.05 to 1 g/L were considered and K_c (as estimated using an equilibrium reversible sorption model and the adsorbed plutonium fraction recorded at $t = 240$ h) generally increased with decreasing C_c.

However, the dimensionless partitioning coefficient K_cC_c appears to be independent of C_c (Table 3). Interestingly, the same also appears to be true for the forward rate α. A working hypothesis, which requires further testing, could therefore be that α is independent of C_c. This, however, could be valid only for sufficiently low plutonium concentrations. Clearly, saturation effects, or the degree to which non-linear sorption is significant, would depend on C_c in relation to dissolved plutonium mass. Such non-linear effects would be more apparent for lower C_c, which if interpreted by the linear model eq 8, would imply smaller α for smaller C_c. If we assume that α is proportional to C_c (assumed in e.g., (11)), then we can define an intrinsic rate as $\alpha_c \equiv \alpha/C_c$ (12). The range of α_c is 0.0017-0.1 L/(g h).

Smectite

The data points for smectite resemble those for hematite: a rapid and relatively large increase of adsorbed Pu fraction ϕ over a short time (up to 24 h) and then a relatively small, linear increase of ϕ between 24 h and 240 h. For this data set, the asymptotic expression eq 10 appears to be a good approximation, as the estimates of K_c and α are based on all four data points (as for silica with $C_c = 0.2$ g/L). The two-site model provides a good match with all but the first data point. By contrast, the one-site data

model provides a poor match with all but two data points (24 h and 240 h, Figure 3 for smectite).

5 Non-uniqueness in the macroscopic interpretation

Short of a full mechanistic microscopic explanation for Pu sorption on the minerals considered in the experiments of Lu et al. (1,2), the macroscopic interpretation provided here by the two-site sorption model is non-unique. Given the relatively limited number of data points for each data set, and the limited duration of the experiments, alternative interpretations (models) could in principle be used to reproduce the data sets of Table 1.

The two-site kinetic model implies that one type of site controls sorption at short times, and another type of site controls sorption at longer times. Considering the data of hematite, silica ($C_c = 0.2$ g/L) and smectite, these clearly exhibit two characteristic slopes of ϕ: a steep slope at short time, and a much flatter slope at intermediate and later time, which is consistent with our two-site interpretation. A similar effect could be obtained, however, by interpreting the sorption process as taking place on one type of site with time-dependent kinetic rates.

To illustrate this point, consider a first-order model

$$\frac{dX}{dt} = -\kappa(t)X \tag{2}$$

where $\kappa(t)$ corresponds to the forward sorption rate, and we assume a simplified case where the reverse rate is negligible over the experimental time of interest. The solution of eq 2 for normalized mass is

$$X(t) = \exp\left[-\int_0^t \kappa(\tau)\, d\tau\right].$$

Say now that $\kappa(t)$ has a simple two-step form of $\kappa = k_f =$ constant for $t < t_*$ and $\kappa = \alpha =$ constant for $t > t_*$, where $k_f > \alpha$. The change of X then exhibits two characteristic slopes, depending on the magnitudes of k_f and α. In particular, for small t_* relative to the experimental duration, and k_f/α large, we would obtain two slopes for X: an initial rapid change and a later gradual change.

6 Detection limits for kinetic rates and their effect on prediction uncertainty

In Figure 1 we showed the potential impact of colloids as a function of dimensionless slow rates α and β. These rates may be difficult to measure in a short-duration experiment, and the ranges for these rates that could be detected in a reasonable time frame is an important consideration for applications. To obtain an estimate of the detection

limit, we first assume that slow desorption is unimportant on the time scale of the experiment and set $\beta = 0$. Since $\beta = 0$ implies a maximum impact of colloids (Figure 1), it is also most interesting for applications. With $\beta \approx 0$, α is the only rate significant for colloid-facilitated transport to be determined from a batch test.

The relevant expression for evaluating a batch test under these conditions is eq 9. Suppose that the error for the dissolved tracer concentration measurement is 1% (consistent with Lu et al. (1,2)). Let the duration of a sorption experiment be t_E. At $t = 0$, we approximate the partitioning as instantaneous, i.e., $X(0) = 1/R_c$ where $R_c = 1 + C_c K_c$. Tracer in solution decreases for $t > 0$ such that $X(0) - X(t_E) > 0$. We set the lower limit to 1% as

$$\frac{X(0) - X(t_E)}{X(t_E)} \leq 0.01$$

and compute the detection limit for α from eq 9 as

$$\alpha_\star = \frac{1}{t_E} \ln(1.01)\, R_c. \tag{3}$$

The detection limit is inversely propotional to the experiment duration and directly proportional to R_c. The limit is also approximately proportional to $K_c C_c$ for large $K_c C_c$. In other words, estimating α from batch tests is more difficult for tracers subject to stronger fast partitioning, because the minimum detectable α in larger. The detection limit is also a weak function of the experimental error, suggesting that improved precision in the measurement of sorbed concentration would have little effect on reducing the detection limit.

Eq 3 is approximate in the sense that fast kinetics and slow desorption are neglected. Clearly, on time scales of laboratory tests the fast kinetics (controlled by k_f and k_r) will generally be observable. Thus depending on the rates k_f and k_r relative to the duration of a batch test, fast kinetics may further increase the uncertainty in estimates of the slow kinetic rates α and β, beyond that anticipated by eq 3.

Detection limits for the slow reverse rate β are also strongly dependent on the experiment duration. The basic assumption of our re-evaluation of the data by Lu et al. (1,2) was that $\beta = 0$, i.e., that the slow kinetics are irreversible. Clearly, the concept of irreversibility is applicable here only in a relative sense (over the experimental time frame). In other words, we assume that $\beta t_E \approx 0$ where $t_E = 240$ h is the duration of the sorption experiments. Although very slow reverse rates may be immaterial in short experiment, they may still have an effect on long-term predictions. An interesting issue then is how the adsorbed Pu fraction could develop for $t > t_E$, depending on the magnitude of β. Such a thought experiment provides some insights into possible uncertainties associated with extrapolation from short experiments to long-term transport predictions.

In Figure 3 we illustrate ϕ for silica with $C_c = 0.2$ g/L and for smectite, assuming an experimental duration of 1000 h, and for different values of β. To generate curves in Figure 4, we used the full batch solution eq 7 given in the Appendix. The largest β considered in Figure 4 is 0.001 1/h, which yields a change of ϕ at $t = 240$ h, approximately within the error margin of 1%. In other words, the change of ϕ would not be observable

for $\beta < 0.001$ 1/h for $t \leq 240$ h. For smaller values of β, the experimental duration required to observe the effect of reversibility would be larger. To observe an effect of reversibility of the slow kinetics at 1000 h of a sorption experiment for silica, a minimum β of approximately 0.00005 1/h would be required (assuming again an error margin of 1%). In other words, for $\beta < 0.00005$ 1/h, sorption for silica would appear irreversible for an experimental duration of 1000 h. The corresponding limit in β for smectite is larger, approximately 0.00015 1/h, following from the fact that $K_c C_c$ for smectite is larger than for silica. This is consistent with eq 3, where for a given experimental duration, a larger detectable limit for α is obtained with increasing $K_c C_c$.

Uncertainties caused by lack of knowledge of the reverse rate β are even larger if we extrapolate from limited duration laboratory experiments to field-scale discharge of Pu using the flow-through solution. For the conditions of the Lu et al. experiments on silica colloids, β can constrained to the range 0-0.001 1/h based on a 1% error margin. Using the value $\alpha = 0.0018$ from Table 3 and a turnover time of 2000 years, we see from Figure 1b that the peak Pu discharge may be enhanced over the equilibrium value by a factor ranging from 2 to 6000, indicating large uncertainty in predicted performance of the geological barrier. This large uncertainty range may be reduced considerably by longer duration experiments that are specifically designed to address desorption effects.

7 Summary and conclusions

As a rule, sorption of actinides on inorganic colloids appears to exhibit kinetic effects. Moreover, equilibrium sorption models do not provide an adequate quantitative framework for interpreting several field observations of colloid-facilitated transport, where indications are that sorption is irreversible or slowly reversible (9,10). There are two relevant issues for applications: (1) how important is sorption kinetics for field scale transport? (2) if it is important, can the relevant rates be inferred on laboratory time scales?

We presented a two-site kinetic sorption model for a flow and batch reactor and provided analytical solutions for several special cases. The proposed model is consistent with the field scale model for colloid-facilitated transport developed by Cvetkovic (12) and is adopted here for interpreting sorption data under laboratory conditions. The key feature of the model is that two types of sites are assumed to be characterized by different kinetic rates: "fast" sites with relatively high rates and "slow" sites with relatively low rates. For limited-duration laboratory experiments, it is often appropriate to neglect the slow reverse rate and treat the slow sorption process as irreversible over the experiment time frame.

Colloid-facilitated transport is one of the few plausible mechanisms that could potentially allow strongly sorbing radionuclides to bypass geological barriers in high-level waste repository systems. However, colloid-facilitated transport is significant only if sorption is kinetically controlled (Figure 1). In particular, the peak of the Pu discharge from the aquifer may be enhanced by several orders of magnitude when compared to the situation without colloids, depending on the magnitude of the slow kinetic rates. The

enhancement is maximum when $\beta = 0$ (irreversible sorption), but the effect of kinetics can be significant for α/β as small as 100 (Figure 1b). Thus an understanding of colloid sorption kinetics is important in assessing the performance of geological barriers in repository systems. It is noted, however, that other physical mechanisms (physical filtration, sorption of colloids on the porous matrix) may attenuate the colloid-facilitated transport.

It is clear that slow kinetic sorption rates will be difficult to detect in a limited-duration laboratory experiment. The expression eq 3 can be used to estimate detection limits as a function of the experiment duration. Comparing Figure 1 and eq 3, it is clear that slow rates requiring long experimental times to detect could still be of potential significance for colloid-facilitated transport. Under the conditions of Figure 1, for example, a forward rate of 2.85 10^{-6} 1/h could enhance the plutonium discharge by as much as a factor of 70, yet such a small rate would be essentially undetectable for experimental times as long as 7000 hours. Although this analysis was generic in nature and based on a hypothesized measurement error of 1%, similar analysis could be used to evaluate specific experimental plans associated with possible future repository license applications. Insights gained through this analysis could also be used in the design of experimental programs. For example, the sensitivity of the colloid-facilitated discharge to the desorption rate β suggests that experiments specifically designed to address desorption of radionuclides from colloids would have great value in reducing prediction uncertainty.

An asymptotic result for sorbed concentration eq 10 provides a robust parameter estimation procedure for sorption kinetic rates in laboratory experiments. Upon using this approach to re-evaluate the Lu et al. (1,2) data sets, we find two of the data sets exhibit convincing indications of kinetic behavior with two widely separated time scales. Specifically, the silica (with $C_c = 0.2$ g/L) and smectite (with $C_c = 1$ g/L) data sets are poorly fitted by a one-site model and well represented by the two-site model. Discrimination between the two models is less apparent for hematite (with $C_c = 0.2$ g/L), and impossible for montmorillonite (with $C_c = 0.2$ g/L). Nevertheless, the two-site model interpretation cannot be excluded for any of the data sets.

The results for silica provide some indications of parameter dependence on colloid concentration. For the two C_c values available (0.2 and 1.0 g/L), the dimensionless partitioning coefficient K_cC_c is nearly independent of C_c. Interestingly, the forward rate α also appears to be independent of C_c, in conflict with the assumption ($\alpha \propto C_c$) used in earlier theoretical studies (e.g., (11,12)). This dependence on C_c is an important issue given the relatively low colloid concentrations found in groundwater. More data addressing the possible dependence on colloid concentration is clearly needed.

Our analysis of the few data sets from Lu et al. (1,2) should be considered preliminary. A comprehensive re-evaluation of the Lu et al. data would need to consider other possible model interpretations (such as time-dependent kinetics, and non-linear effect) and would need to analyze both the sorption and desorption experiments. Most importantly, for a complete interpretation of Lu et al. data, we need to better understand the microscopic exchange mechanisms of Pu on inorganic colloids, as they take place on different time

scales. Interesting issues in this context are whether the mechanistic basis for slow kinetics is more physical (diffusion) or chemical (e.g., immobilization) in nature, and how the macroscopic fast and slow rates can be related to independently observable microscopic phenomena.

Whatever the actual microscopic mechanisms, they are presumably complex. The current model provides a macroscopic phenomenological representation applicable on the laboratory scale, and is thus a simplification of the microscopic reality. The model is not expected to entirely reproduce any data set. The proposed model may nevertheless be useful for interpreting laboratory data where indications are found for kinetic behavior occurring on two widely separated time scales similar to the data of Lu et al. (1,2). Related models (12) may also be useful in extrapolation to the field scale in a safety and risk assessment context.

Acknowledgments

This paper documents work performed by the Center for Nuclear Waste Regulatory Analyses under contract No. NRC-02-97-009. The work is an independent product and does not necessarily reflect the regulatory position of the NRC. The authors are grateful to Drs. B. Sagar and C. Dinwiddie for their careful review of the manuscript.

Appendix: Analytical solutions

The general solution of eq 1 is obtained in the Laplace domain as

$$\widehat{X} = M_0\,\widehat{\varphi}\left[\frac{(s'+\omega+k_r)(s'+\omega+\beta)}{(s'R+\omega+k_f+\alpha)(s'+\omega+\beta)(s'+\omega+k_r)-\alpha\beta(s'+\omega+k_r)-k_fk_r(s'+\omega+\beta)}\right]$$

$$\widehat{Y} = \frac{k_f}{s'+\omega+k_r}\widehat{X} \tag{4}$$

$$\widehat{Z} = \frac{\alpha}{s'+\omega+\beta}\widehat{X}$$

where $s' \equiv s+\lambda$, s is the Laplace transform variable, and the "hat" denotes Laplace transform.

In the following, we normalize X, Y and Z with M_0, and for simplicity retain the same notation. Thus if $\omega, \lambda = 0$, $RX + Y + Z = 1$. Also, we consider only injection conditions where $\widehat{\varphi} = 1$, or $\varphi(t) = \delta(t)$.

In the general situation, the concentrations can be obtained as functions of time by numerical inverse Laplace transform of eq 4. In special cases of interest in the present discussion, closed form solutions can be obtained as described in the following subsections.

Flow reactor

When fast sorption rates are sufficiently large relative to the turnover time, i.e., $k_f/\omega, k_r/\omega \gg 1$, eq 4 reduces to (for $\lambda = 0$)

$$\widehat{X} = \frac{s+\omega+\beta}{(sR+\omega R_c+\alpha)(s+\omega+\beta)-\alpha\beta}$$

$$\widehat{Y} = C_c K_c \widehat{X} \tag{5}$$

$$\widehat{Z} = \frac{\alpha}{s+\omega+\beta}\widehat{X}$$

where $R_c = 1 + K_c C_c$.

Inversion yields

$$R\,X(t) = \frac{1}{2}\,\mathrm{e}^{(b-a/2)t} + \frac{1}{2}\,\mathrm{e}^{-(b+a/2)t} + \frac{1}{2b}\left(\omega+\beta-\frac{a}{2}\right)\left[\mathrm{e}^{(b-a/2)t} - \mathrm{e}^{-(b+a/2)t}\right]$$

$$Y(t) = C_c K_c X(t) \quad ; \quad Z(t) = \alpha\left[\mathrm{e}^{-(\beta+\omega)\,t} * X(t)\right] \tag{6}$$

where

$$a \equiv \omega+\beta+\omega\frac{R_c}{R}+\frac{\alpha}{R} \quad ; \quad b^2 \equiv \frac{a^2}{4} - \omega\beta\frac{R_c}{R} - \omega^2\frac{R_c}{R} - \omega\frac{\alpha}{R}$$

and "*" denotes convolution. If λ is finite, expressions for $X(t)$ and $Z(t)$ should be multiplied by $\mathrm{e}^{-\lambda t}$.

Batch reactor

The conditions for a batch reactor are obtained from eq 4 by setting $\omega = 0$. With initial conditions

$$X = 1 \quad ; \quad Y = 0 \quad ; \quad Z = 0 \quad \text{for} \quad t = 0$$

and assuming $\lambda = 0$, inversion yields

$$X(t) = f(t) + \beta\,F(t) \tag{7}$$

where

$$f(t) = \frac{1}{2}\,\mathrm{e}^{(b-a/2)t} + \frac{1}{2}\,\mathrm{e}^{-(b+a/2)t} + \frac{1}{2b}\left(k_r-\frac{a}{2}\right)\left[\mathrm{e}^{(b-a/2)t} - \mathrm{e}^{-(b+a/2)t}\right]$$

$$F(t) = \frac{1}{2(b-a/2)}\left[\mathrm{e}^{(b-a/2)t}-1\right] + \frac{1}{2(b+a/2)}\left[1-\mathrm{e}^{-(b+a/2)t}\right] +$$
$$\frac{1}{2b}\left(k_r-\frac{a}{2}\right)\left\{\frac{1}{b-a/2}\left[\mathrm{e}^{(b-a/2)t}-1\right] - \frac{1}{b+a/2}\left[1-\mathrm{e}^{-(b+a/2)t}\right]\right\}$$

$$a \equiv k_f + k_r + \alpha + \beta \quad ; \quad b^2 \equiv \frac{a^2}{4} - k_f\beta - k_r\,\alpha - k_r\beta.$$

If the reverse rate of the slow sites β is small relative to the considered experimental time, i.e., $\beta \to 0$, we obtain the solution for the irreversible limit as

$$X(t) = \frac{1}{2}\,\mathrm{e}^{(b-a/2)t} + \frac{1}{2}\,\mathrm{e}^{-(b+a/2)t} + \frac{1}{2b}\left(k_r - \frac{a}{2}\right)\left[\mathrm{e}^{(b-a/2)t} - \mathrm{e}^{-(b+a/2)t}\right] \tag{8}$$

where

$$a \equiv k_f + k_r + \alpha \quad ; \quad b^2 \equiv \frac{a^2}{4} - k_r\,\alpha.$$

Of particular interest is the asymptotic result for times sufficiently large such that sorption on fast sites may be considered at equilibrium. Then we have

$$X(t) = \frac{1}{1 + K_c C_c}\,\exp\left(-\frac{\alpha t}{1 + K_c C_c}\right) \tag{9}$$

where K_c [L/g] is the equilibrium partitioning coefficient, and C_c [g/L] is the colloid concentration.

For small arguments $\alpha t/(1 + K_c C_c)$, we expand the exponential in eq 9 to obtain a simple expression for the adsorbed fraction $\phi(t) = 1 - X(t)$

$$\phi(t) \approx \frac{K_c C_c}{1 + K_c C_c} + \frac{\alpha\, t}{(1 + K_c C_c)^2} \tag{10}$$

whereby the adsorbed tracer fraction increases linearly with time.

Literature Cited

(1) Lu, N.; Triay, I. R.; Cotter, C. R.; Kitten, H. D.; Bentley, J. Reversibility of sorption of Plutonium-239 onto colloids of Hematite, Goethite, Smectite and Silica: A milestone final report of YMP. Technical Report LA-UR-98-3057, Los Alamos National Laboratory, 1998.

(2) Lu, N.; Conca, J.; Parker, G. A.; Leonard, P. A.; Moore, B.; Strietelmeier, B.; Triay, I. R. Adsorption of actinides onto colloids as a function of time, temperature, ionic strength, and colloid concentration. Technical Report LA-UR-00-5121, Los Alamos National Laboratory, 2000.

(3) Corapcioglu, M.Y.; Jiang, S. *Water Resour. Res.*, **1993**, *29*, 2215–2226.

(4) Honeyman, B. D. *Nature*, **1999**, *397*, 23–24.

(5) Ouyang, Y.; Shinde, D.; Mansell, R.S.; Harris, W. *Crit. Rev. Environ. Sci. Technol.*, **1996**, *26*, 189–204.

(6) *Disposition of high-level radioactive waste through geological isolation: development, current status, and technical and policy challenges.* Prepared by: National Research Council, 1999.

(7) *Total system performance assessment for the site recommendation.* Technical Report TDF-WIS-PA-00001 REV 00, Prepared for U.S. Department of Energy; Prepared by Civilian Radioactive Waste Management System Management and Operating Contractor, 2000.

(8) *Yucca Mountain science and engineering report: Technical information supporting site recommendation consideration.* Technical Report DOE/RW-0539. Prepared for U.S. Department of Energy; Prepared by U.S. Department of Energy Yucca Mountain Site Characterization Office. 2001.

(9) Penrose, W. R.; Polzer, W. L.; Essington, E. H.; Nelson, D. M.; Orlandini, K. A. *Environ. Sci. Technol.*, **1990**, *24*, 228–234.

(10) Kersting, A. B.; Efured, D. W.; Finnegan, D. L. ; Rokop, D. J.; Smith, D. K.; Thompson, J. L. *Nature*, **1999**, *397*, 56–59.

(11) Saiers, J. E.; Hornberger, G. M. *Water Resour. Res.*, **1996**, *32*, 33–41.

(12) Cvetkovic, V. *Phys. Fluids*, **2000**, *12*, 2279–2294.

(13) Painter, S.; Cvetkovic, V.; Turner, D. R. *Ground Water*, **2001**, *39*(3), 326–338.

Figure captions

Figure 1: Potential effect of slow sorption kinetics on transport of Pu through a flow reactor. The basic transport parameters for the flow reactor are chosen to be consistent with previous representations of the alluvial aquifer near Yucca Mountain, Nevada (13,12): $\omega = 1/ < \tau >$ where $< \tau >= 4000$ yr is the mean residence time in the aquifer, $K_d = 5$ L/g, $\theta = 0.3$, $\rho = 2400$ kg/m^3 and Pu half-life of 2.4×10^4 yr. (a) Total Pu discharge for different rates $\alpha < \tau >$ and normalized to the total discharge without colloids $X_{eq}(t) = X_0 \exp(-\omega t/R - \lambda t)$; (b) peak of normalized total Pu discharge for different forward $\alpha < \tau >$ and reverse $\beta < \tau >$ rates.

Figure 2: Comparison of one- and two-site sorption model interpretations of five data sets for Pu sorption on four colloid types (minerals) reported in Lu et al. (1,2).

Figure 3: Effect of the slow reverse rate β on the possible change of the adsorbed Pu fraction for silica and smectite beyond the experimental time of 240 h. This plot illustrates the uncertainties inherent in extrapolating from short-duration sorption experiments.

Table 1: Adsorbed plutonium fraction as a function of time for four minerals and five cases, from Lu et al. (1,2).

Time [h]	Hematite ($C_c = 0.2$ g/L) ϕ	Montmorillonite ($C_c = 0.2$ g/L) ϕ	Silica ($C_c = 0.2$ g/L) ϕ	Smectite ($C_c = 1$ g/L) ϕ	Silica ($C_c = 1$ g/L) ϕ
1	0.495±0.002	0.044±0.0036	0.023 ±0.0014	0.553±0.006	0.189 ±0.005
4	0.722±0.011	0.081±0.024	0.254±0.105	0.637±0.002	0.3 ±0.028
24	0.821±0.012	0.141±0.012	0.524±0.004	0.809±0.0	0.364 ±0.011
48	0.938±0.0045	0.167±0.0038	0.537±0.008	0.838±0.011	0.431±0.009
96	0.951±0.007	0.444±0.04	0.57 ±0.00074	0.86±0.008	0.58±0.003
240	0.956±0.0016	0.537±0.043	0.618±0.0006	0.899±0.003	0.62±0.001

Table 2: Summary of estimated parameters for the 1-site model.

Mineral	Estimated using eq 8 with $\alpha = 0$		Computed $k_f/(k_r C_c)$	Equilibrium (Lu et al.)
	k_f [1/h]	k_r [1/h]	K_c [L/g]	K_c [L/g]
Hematite ($C_c = 0.2$ g/L)	0.25	0.014	89	110
Montmor. ($C_c = 0.2$ g/L)	0.0095	0.008	6	5.8
Silica ($C_c = 0.2$ g/L)	0.026	0.016	8.1	8.1
Smectite ($C_c = 1$ g/L)	0.1	0.012	8.3	6.4
Silica ($C_c = 1$ g/L)	0.0183	0.011	1.7	1.5

Table 3: Summary of estimated parameters K_c, α and k_r for the 2-site model.

Mineral	Estimated using eq 10			Calibrated using eq 8	Computed $k_r K_c C_c$
	Number of data points	α [1/h]	K_c [L/g]	k_r [1/h]	k_f [1/h]
Hematite ($C_c = 0.2$ g/L)	3	0.02	76	0.012	0.182
Montmor. ($C_c = 0.2$ g/L)	2	0.0017	3.1	0.02	0.012
Silica ($C_c = 0.2$ g/L)	4	0.0018	5.4	0.1	0.108
Smectite ($C_c = 1$ g/L)	4	0.0107	4.4	0.06	0.264
Silica ($C_c = 1$ g/L)	–	0.0018	1.1	0.035	0.039

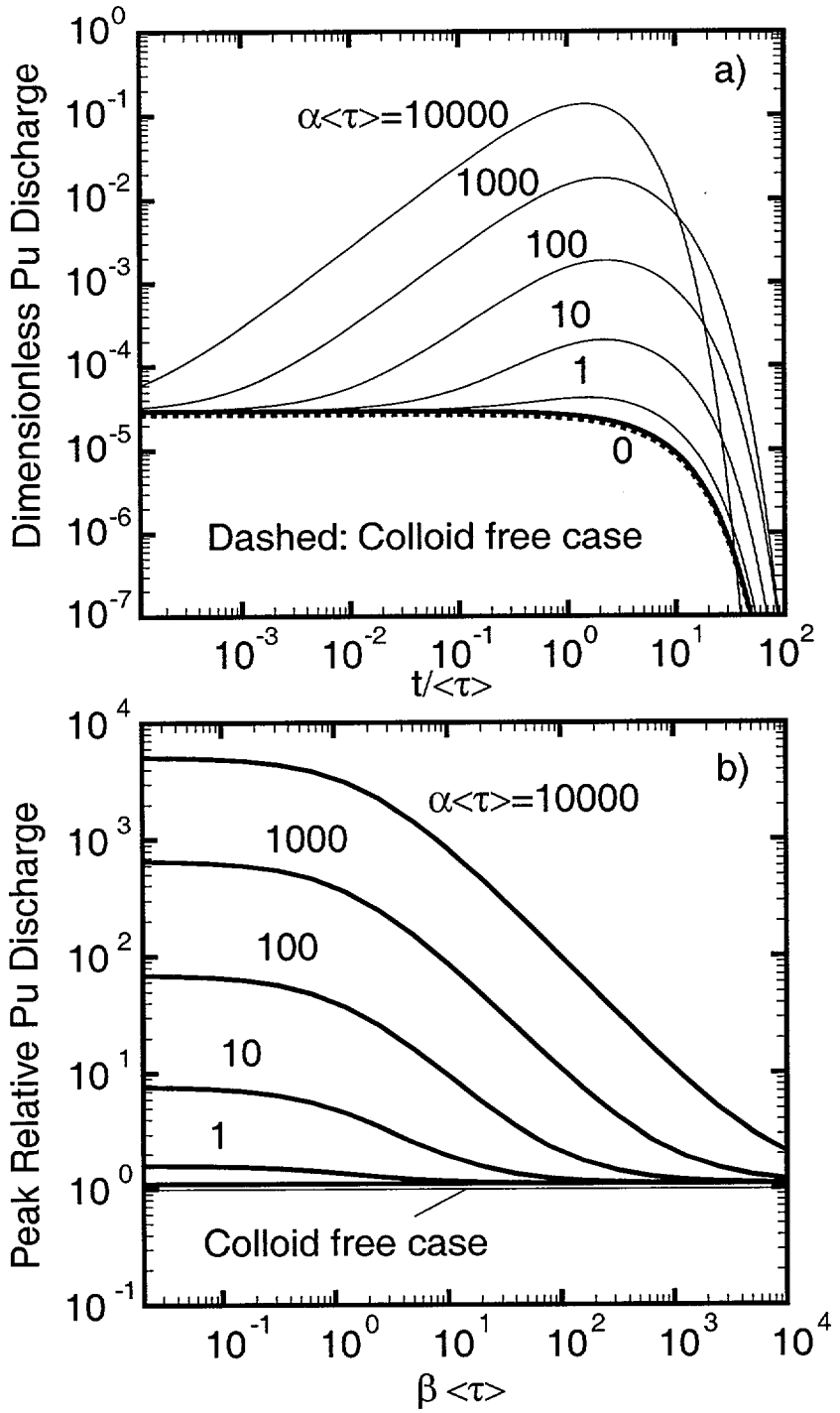
a)
Dimensionless Pu Discharge
α<τ>=10000
1000
100
10
1
0
Dashed: Colloid free case
t/<τ>
b)
Peak Relative Pu Discharge
α<τ>=10000
1000
100
10
1
Colloid free case
β <τ>

Figure 1

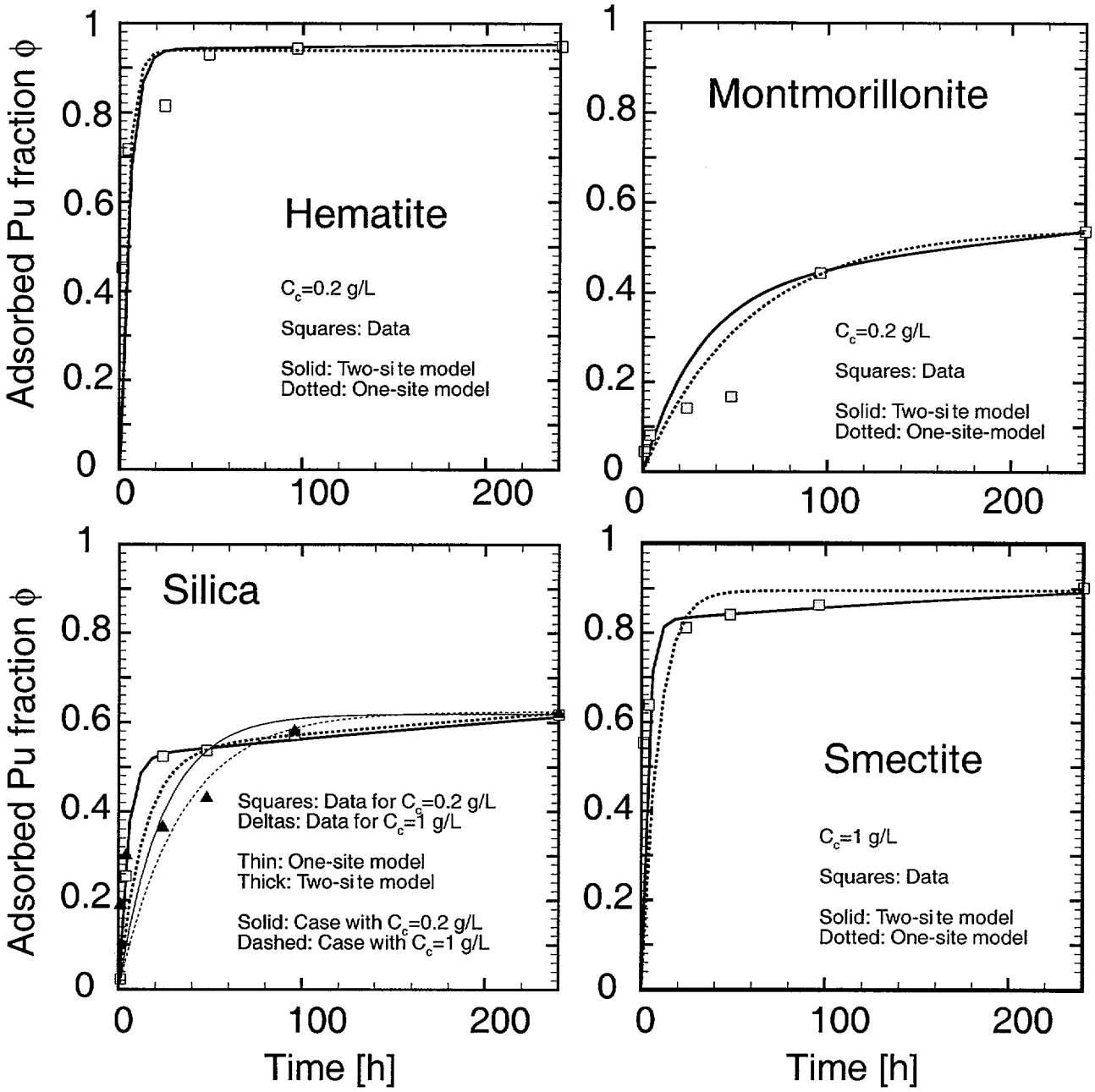
Hematite
C_c=0.2 g/L
Squares: Data
Solid: Two-site model
Dotted: One-site model
Montmorillonite
C_c=0.2 g/L
Squares: Data
Solid: Two-site model
Dotted: One-site-model
Silica
Squares: Data for C_c=0.2 g/L
Deltas: Data for C_c=1 g/L
Thin: One-site model
Thick: Two-site model
Solid: Case with C_c=0.2 g/L
Dashed: Case with C_c=1 g/L
Smectite
C_c=1 g/L
Squares: Data
Solid: Two-site model
Dotted: One-site model
Adsorbed Pu fraction ϕ
Time [h]
0
0.2
0.4
0.6
0.8
1
100
200

Figure 2

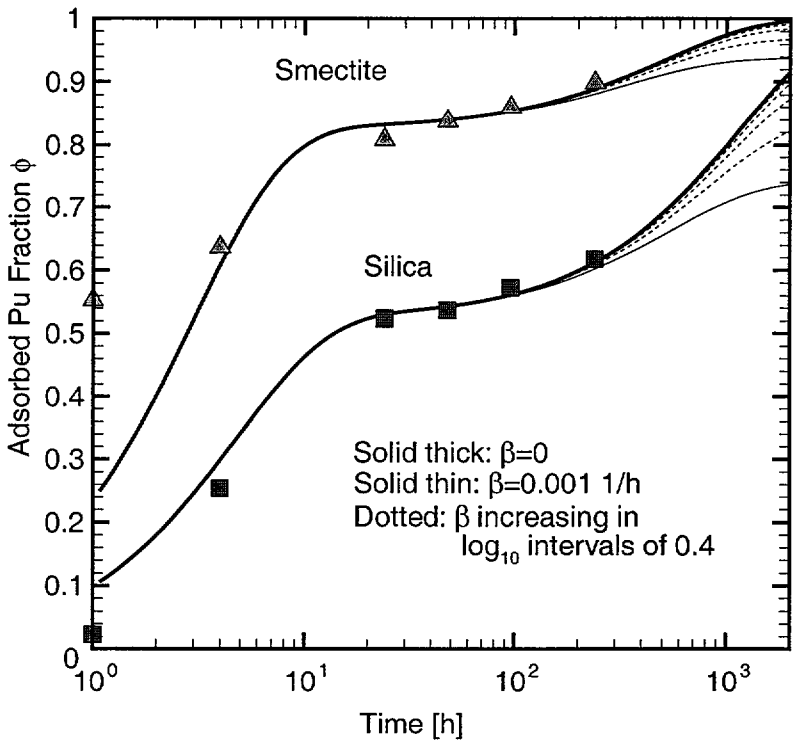
Smectite
Silica
Solid thick: β=0
Solid thin: β=0.001 1/h
Dotted: β increasing in
log10 intervals of 0.4
Adsorbed Pu Fraction ϕ
Time [h]
0
0.1
0.2
0.3
0.4
0.5
0.6
0.7
0.8
0.9
1
10^0
10^1
10^2
10^3

Figure 3